◆ Human Brain Mapping 36:3761–3776 (2015) ◆

Altered Amygdalar Resting-State Connectivity in Depression is Explained by Both Genes and Environment

Aldo Córdova-Palomera,[1,2] Cristian Tornador,[3] Carles Falcón,[4,5] Nuria Bargalló,[2,4,6] Igor Nenadic,[7] Gustavo Deco,[3,8] and Lourdes Fañanás[1,2]*

[1]*Unidad de Antropología, Departamento de Biología Animal, Facultad de Biología and Instituto de Biomedicina (IBUB), Universitat de Barcelona, Barcelona, Spain*
[2]*Centro de Investigaciones Biomédicas en Red de Salud Mental (CIBERSAM), Madrid, Spain*
[3]*Center for Brain and Cognition, Computational Neuroscience Group, Department of Information and Communication Technologies, Universitat Pompeu Fabra, Barcelona, Spain*
[4]*Medical Image Core facility, the Institut d'Investigacions Biomèdiques August Pi i Sunyer (IDIBAPS), Barcelona, Spain*
[5]*Centro de Investigación Biomédica en Red en Bioingeniería, Biomedicina y Nanomedicina (CIBER-BBN), Zaragoza, Spain*
[6]*Centro de Diagnóstico por Imagen, Hospital Clínico, Barcelona, Spain*
[7]*Department of Psychiatry and Psychotherapy, Jena University Hospital, Friedrich Schiller University Jena, Jena, Germany*
[8]*Institució Catalana de la Recerca i Estudis Avançats (ICREA), Universitat Pompeu Fabra, Barcelona, Spain*

Abstract: Recent findings indicate that alterations of the amygdalar resting-state fMRI connectivity play an important role in the etiology of depression. While both depression and resting-state brain activity are shaped by genes and environment, the relative contribution of genetic and environmental factors mediating the relationship between amygdalar resting-state connectivity and depression remain largely unexplored. Likewise, novel neuroimaging research indicates that different mathematical representations of resting-state fMRI activity patterns are able to embed distinct information relevant to brain health and disease. The present study analyzed the influence of genes and environment on

Additional Supporting Information may be found in the online version of this article.

Aldo Córdova-Palomera and Cristian Tornador contributed equally to this work.

Contract grant sponsor: Spanish; Contract grant number: SAF2008-05674-C03-01; Contract grant sponsor: European Twins Study Network on Schizophrenia Research Training Network; Contract grant number: EUTwinsS, MRTN-CT-2006-035987; Contract grant sponsor: Catalan; Contract grant number: 2014SGR1636; Contract grant sponsor: Ministry of Science and Innovation in frame of ERA-NET NEURON; Contract grant number: PIM2010ERN-00642; Contract grant sponsor: ERC Advanced Grant DYSTRUCTURE; Contract grant number: 295129; Contract grant sponsor: FET Flagship Human Brain Project; Contract grant number: 604102; Contract grant sponsor: Spanish Government; Contract grant number: PSI2013-42091; Contract grant sponsor: FP7-ICT BrainScaleS; Contract grant number: 269921; Contract grant sponsor: CORONET; Contract grant number: 269459; Contract grant sponsor: EraNet Neuron SEMAINE; Contract grant number: PCIN-2013-026.

*Correspondence to: Prof. Dr. Lourdes Fañanás Saura, Unitat d'Antropologia, Departamento de Biologia Animal, Facultat Biologia, Universitat de Barcelona, Av. Diagonal, 645. Barcelona 08028, Spain. E-mail: lfananas@ub.edu

Received for publication 7 February 2015; Revised 5 May 2015; Accepted 2 June 2015.

DOI: 10.1002/hbm.22876

Published online 19 June 2015 in Wiley Online Library (wileyonlinelibrary.com).

amygdalar resting-state fMRI connectivity, in relation to depression risk. High-resolution resting-state fMRI scans were analyzed to estimate functional connectivity patterns in a sample of 48 twins (24 monozygotic pairs) informative for depressive psychopathology (6 concordant, 8 discordant and 10 healthy control pairs). A graph-theoretical framework was employed to construct brain networks using two methods: (i) the conventional approach of filtered BOLD fMRI time-series and (ii) analytic components of this fMRI activity. Results using both methods indicate that depression risk is increased by environmental factors altering amygdalar connectivity. When analyzing the analytic components of the BOLD fMRI time-series, genetic factors altering the amygdala neural activity at rest show an important contribution to depression risk. Overall, these findings show that both genes and environment modify different patterns the amygdala resting-state connectivity to increase depression risk. The genetic relationship between amygdalar connectivity and depression may be better elicited by examining analytic components of the brain resting-state BOLD fMRI signals. *Hum Brain Mapp 36:3761–3776, 2015.*

Key words: amygdala; resting-state fMRI; environment; depression; signal processing; Hilbert transform; MZ twins

INTRODUCTION

Depressive disorders are becoming one of the leading causes of economic burden globally [Murray et al., 2012], with lifetime prevalence estimates reaching up to 20% in some cases [Kessler et al., 2007]. It is generally accepted that depression can partly be traced back to environmental factors such as adverse childhood familial environment, personality traits and stressful adult life events, among others [Kendler et al., 2003; Moffitt et al., 2007]. Likewise, research has demonstrated that an important extent of the risk for this psychopathological disorder can be explained by genetic influences and by the synergic effect of genes and environment [Domschke and Reif, 2012; Leonardo and Hen, 2006; Sullivan et al., 2000].

In this sense, parsing out genes and environment has enormous importance in the search for the etiological origins of mental disorders, as (i) it has been suggested that some alternative phenotypes (i.e., endophenotypes) may have a stronger link to the genetic basis of psychopathology than phenomenologically-derived clinical diagnoses [Glahn et al., 2014; Gottesman and Gould, 2003] and (ii) the identification of non-genetic influences on psychiatric conditions has several epidemiological and public health implications [Duncan and Keller, 2011; Freeman and Stansfeld, 2008; Lundberg, 1998].

Importantly, neuroimaging studies may provide an important reference framework to understand such complex multifactorial basis of disease [Blokland et al., 2012; Hyde et al., 2011; Paus, 2013], and research has shown that resting-state functional magnetic resonance imaging (fMRI) brain network alterations may serve as endophenotypic markers of neuropsychiatric disorders [Glahn et al., 2010].

Novel findings on the genetics of the connectome have pointed out that resting-state functional brain connectivity, as measured by blood-oxygen-level dependent (BOLD) fMRI signals, is influenced by both genes and environment. Specifically, three quantitative genetic studies have reported on the heritability of important resting-state fMRI network features. Glahn et al. [2010] analyzed data of 333 individuals from 29 families to conclude that several features of the default mode network are partly heritable and may be used as endophenotypic measures for psychiatric disorders. In addition, Fornito et al. [2011] examined a sample of 16 monozygotic (MZ) and 13 dizygotic adult twin pairs, and found strong genetic influences on global network efficiency. Likewise, a more recent report by van den Heuvel et al. [2013] using a sample of 21 MZ and 22 dizygotic twin pairs; their main findings indicate an important role for genetic factors on global network metrics of the resting brain. While these three reports constitute sound evidence of large genetic influences–as well as unique environmental factors–underlying BOLD fMRI connectivity patterns during rest, they have mainly focused on global network measures at either the whole-brain or the default mode network in healthy individuals. Complementarily, studies of candidate genes in samples of genetically unrelated individuals have suggested a role for genes such as *ZNF804A*, *APOE*, *COMT*, and *MET* as modulators of different resting-state fMRI network parameters in neuropsychiatric phenotypes such as Alzheimer's disease, schizophrenia and autism [Esslinger et al., 2011; Filippini et al., 2009; Liu et al., 2009; Martin et al., 2014; Rudie et al., 2012; Trachtenberg et al., 2012; Tunbridge et al., 2006].

Overall, these ample evidences indicate that resting-state networks extracted from BOLD fMRI measurements have separate genetic and environmental influences. Likewise, they suggest that the association between some specific genetic or environmental factors and several psychopathological outcomes may be mediated by the disruption of the resting-state networks. Despite this, to the best of our knowledge, no previous study has evaluated the potential genetic or environmental etiology of the resting-state fMRI network alterations underlying depressive disorders. This is an important issue, as recent studies of have consistently

shown alterations of the resting-state fMRI activity patterns in depressed individuals [Dutta et al., 2014].

Specifically, one of the most consistently replicated finding in resting-state fMRI studies of depression is a disruption of the amygdalar activity [Cullen et al., 2014; Dutta et al., 2014; Wang et al., 2014; Zeng et al., 2014]. Briefly, these recent reports have shown alterations of amygdalar connectivity in adolescent depression [Cullen et al., 2014]; disrupted connectivity strength in major depressive disorder patients who previously suffered childhood neglect [Wang et al., 2014]; and important amygdalar modifications that may serve to discriminate a depressed from a healthy brain [Zeng et al., 2014].

Other alterations of the amygdalar activity in resting-state fMRI networks of depressed individuals have widely been described across the literature [Dutta et al., 2014]. For instance, a number of disruptions in the affective network comprising the amygdala, the hippocampus and related regions have been found in depression [Zeng et al., 2012; Zhang et al., 2014a]. These results are somehow consistent with the findings by Sheline and colleagues, who described alterations in sets of brain regions comprising the amygdala, such as the affective and the default mode networks [Sheline et al., 2009, 2010]. Similarly, network alterations of pathways connecting the amygdala and the prefrontal cortex have been found after selective serotonin reuptake inhibitor antidepressant treatment [McCabe and Mishor, 2011]. Overall, these and other related studies support the idea of a disruption of amygdalar resting-state connectivity as one of the main mechanisms underlying large-scale network disruptions in depression [Kaiser et al., 2015].

These resting state connectivity alterations index modifications in the communication between the amygdala and a wide set of regions across the whole brain. In the context of large-scale networks, these disruptions may be thought of as changes in the information processing mechanisms between the amygdala and other cerebral structures [van den Heuvel and Hulshoff Pol, 2010]. It is worth mentioning that resting-state communication between regions can be understood from several alternative viewpoints, some of which have–at least in principle–their own potential relevance in clinical settings [Lee et al., 2013]. Among numerous methods to study brain activity at rest, one of the most promising approaches is the assessment of the spatio-temporal patterns of coactivation between regions through network modeling [Richiardi et al., 2011; Smith, 2012; van den Heuvel and Hulshoff Pol, 2010]. Conventionally, low-frequency periodic time courses of resting-state activation patterns are extracted from a set of anatomical regions, and strong first-order correlations in the temporal configuration of activity between two anatomically separated regions is abstracted as a functional connection [De Vico Fallani et al., 2014; van den Heuvel and Hulshoff Pol, 2010].

While this method of extracting networks from correlated temporal activity between brain regions has undoubtedly led to outstanding neurobiological and clinical findings [Lee et al., 2013], it is essential recognizing that periodic waves can carry information via several different coding systems, some of which constitute the basis of standard devices in communications theory and related technical disciplines [O'Reilly, 1984]. In effect, there is compelling evidence that higher-order brain function may be tightly related to neural communication emerging from the coherent oscillatory activity of the brain regions at specific frequencies [Fries, 2005, 2009]. Namely, information can efficiently be coded and transmitted within different components of neuronal activity waves, which are not straightforwardly deduced by examining its raw time course.

For instance, a common method to analyze brain signals in magnetoencephalography and electroencephalography is the estimation of their analytical representation, which allows transforming one time function—a magnetic or an electric wave recorded over time—into two time functions with meaningful mathematical properties. Of note, novel neuroimaging research has shown that distinct properties of wave-like temporal patterns of fMRI brain activity are able to embed information of particular biological relevance [Glerean et al., 2012], which may have implications for depression [Liu et al., 2014]. It is important noting that recent findings indicate that analytic properties such as the phase or the amplitude envelope of resting-state fMRI oscillations may explain an important extent of the relationship between brain structure and function [Glerean et al., 2012; Guggisberg et al., 2014; Ponce-Alvarez et al., 2015], suggesting such properties could be feasible endophenotype candidates in depression.

Considering these elements, the current study was aimed at determining the relevance of genetic and environmental factors leading to depression by altering amygdalar resting-state fMRI activity. To do so, whole brain resting-state fMRI time series were extracted from a group of 48 MZ twins (24 pairs) informative for depressive psychopathology. Insofar as members of a monozygotic (MZ) twin pair have almost identical DNA sequences, this work studied their phenotypic similarities and differences to obtain insights on familial and environmental influences. Different centrality measures of amygdalar connectivity were estimated by constructing whole-brain networks from resting-state time series, using two distinct methodologies: (i) the conventional examination of correlations between band-pass filtered time series [Smith et al., 2013] and (ii) a technique for extracting analytical components of fMRI signals, which is able to explain a considerable extent of the relationship between brain morphology and resting-state fMRI activity [Glerean et al., 2012; Ponce-Alvarez et al., 2015].

METHODS

Sample Description

The present sample was gathered from a set of 115 Spanish Caucasian adult twin pairs (230 individuals) from

the general population, who gave permission to be contacted for research purposes. All twins were contacted by telephone and invited to participate in a general study of adult cognitive and psychopathological traits. A battery of psychological and neurocognitive tests was administered to the twins by trained psychologists. Similarly, they were interviewed for medical records. Exclusion criteria applied were age under 18 and over 65 years, current substance misuse or dependence, a medical history of neurological disturbance and presence of sensory or motor alterations. Written informed consent was obtained from all participants after a detailed description of the study aims and design, approved by the local Ethics Committee. All procedures were carried out in accordance with the Declaration of Helsinki.

Zygosity of all pairs was assessed by genotyping 16 highly polymorphic microsatellite loci from DNA samples (SSRs; PowerPlex® 16 System Promega Corporation). Identity on all the markers can be used to assign monozygosity with greater than 99% accuracy [Guilherme et al., 2009]. In the whole sample (115 twin pairs), 86 duos were MZ.

From that group of participants, using the previously collected data, a subset of 54 individuals (27 MZ twin pairs) was selected, as they were informative for obstetric and psychopathological traits and gave consent to participate in the MRI part of the present study.

Twins included in this subset of 54 participants met the following criteria: (a) age at scan between 20 and 56 years, (b) both twins right-handed, and (c) none of the twins manifested liability for DSM-IV-R psychiatric diagnoses other than depression and/or anxiety. Pairs where one or both twins manifested either neurological or major medical illnesses were excluded as well (see Measures).

After this point, due to image artifacts or lack of data about six participants, the final sample (i.e., the subset included in all statistical analyses) consisted of 48 individuals (20 males, mean age: 33.6 years).

Psychometric Measures

To evaluate liability for psychopathology in this general population sample, a clinical psychologist applied the Structural Clinical Interview for DSM-IV Axis I Disorders (SCID-I) [First, 1997] in a face-to-face interview to screen for presence of any lifetime psychiatric disorder.

Participants were asked to report if they had received pharmacological or psychological treatment or had consulted a psychiatrist or psychologist as they first participated in the study. Only one individual had life-time exposure to psychopharmacological treatment for depression. However, excluding this individual from the group analyses did not change the significance of the results.

A clinical psychologist applied the Structural Clinical Interview for DSM-IV Axis I Disorders (SCID-I) in a face-to-face interview to screen for the presence of any lifetime depression or related anxiety spectrum disorder. In this sample, six individuals with a history of (mainly) anxious psychopathology were included in the psychopathology-affected group. This apparently broad category of outcomes was used in conjunction with evidence on the comorbidity, shared etiopathology and diagnostic criteria overlap between depressive and anxious disorders [Mosing et al., 2009; Ressler and Mayberg, 2007; Wittchen et al., 2002; Zbozinek et al., 2012], as well as taking into account evidences of amygdalar resting-state alterations across both diagnoses [Oathes et al., 2014]. Remarkably, repeating the statistical analyses removing predominantly anxious individuals did not alter the significance of the results.

Overall, there were ten healthy pairs, six concordant and eight discordant pairs for lifetime DSM-IV diagnoses. Additionally, current depression status and other psychiatric symptoms were evaluated using the Brief Symptom Inventory (BSI) [Derogatis and Melisaratos, 1983; Ruiperez et al., 2001]. The BSI is a self-administered 46-item screening instrument aimed at identifying the experience of psychopathological symptoms during the last 30 days. It is composed by six subscales (depression, phobic anxiety, paranoid ideation, obsession-compulsion, somatization, and hostility) conceived for use in both clinical and nonclinical samples. Items are rated on a five-point scale of distress, according to self-perception of symptoms. Descriptive data from the current sample is summarized in Table I. As shown, all diagnostic concordant pairs were females, and twins with no lifetime history of DSM-IV diagnosis had lower BSI scores—fewer self-reported symptoms—in both the depressive subscale and the whole questionnaire. In addition, neurocognitive data for this sample was collected using the Wechsler Adult Intelligence Scale [Sattler, 2001; Wechsler et al., 1997]. The intelligence quotient (IQ) was estimated from five subtests (block design, digit span, matrix reasoning, information and vocabulary) of this battery. As shown in Table I, IQ scores were similar to those from demographically similar samples [Lynn and Meisenberg, 2010]; of note, there were no intra-group differences in IQ, indicating that neurocognitive influences on resting-state brain signals [Douw et al., 2011; Wang et al., 2011] are not likely to influence subsequent statistical analyses.

MRI Acquisition and Preprocessing

The images were acquired at the MRI Unit of the Image Platform (IDIBAPS, Hospital Clínic de Barcelona), using a TIM TRIO 3 T scanner with an 8-channel head coil (Siemens, Erlangen, Germany). Resting-state fMRI data comprised 210 echo-planar (EPI) BOLD sensitive volumes (TR = 2790 ms, TE = 30 ms, 45 axial slices parallel to anterior-posterior commissure plane acquired in interleaved order, 3.0 mm slice thickness and no gap, FOV = 2075 × 1344 mm^2, voxel size = 2.67 × 2.67 × 3 mm^3).

Additionally, high resolution 3D structural datasets were obtained for anatomical reference, using a T1-weighted magnetization prepared rapid gradient echo, with the following parameters: 3D T1-weighted MPRAGE sequence, TR = 2300

TABLE I. Demographic, psychopathological and neurocognitive data for DSM-IV diagnostic concordant, discordant, and healthy MZ twin pairs

	Concordant (12 subjects, 10 female)		Discordant (16 subjects, 10 female)		Healthy (20 subjects, 8 female)		Group comparison X-squared[a]; *P*
	Mean (SD)	Range	Mean (SD)	Range	Mean (SD)	Range	
Age	42.5 (13)	22–54	37 (10.9)	20–50	30.3 (7.3)	19–39	5.9; 0.052
IQ	105.1 (12.5)	87–127	108.1 (11.8)	87–131	110.5 (5.5)	103–118	1.9; 0.393
Current psychopathology (total BSI)	27.9 (16.5)	6–57	20.9 (13.3)	4–45	10.6 (9.3)	1–33	8.7; 0.013[b]
Current depressive symptoms (BSI subscale)	6.9 (6.5)	1–20	3.5 (2.7)	0–9	1.7 (1.8)	0–6	6.4; 0.04[b]

Notes: SD, standard deviation; IQ, intellectual quotient; BSI, Brief Symptom Inventory
[a]Kruskal–Wallis X-squared, as these variables were continuous
[b]Statistically significant *P*-value

ms, TE = 3.03 ms, TI = 900 ms, Flip angle = 9°, 192 slices in the sagittal plane, matrix size=256 × 256, 1 mm^3 isometric voxel.

Resting-sate time series were obtained by means of standard image processing protocols implemented in the Statistical Parametric Mapping software, version 8 (SPM8) [Friston et al., 1995], running under MATLAB (The Mathworks, Natick, MA). Briefly, after correction of slice-timing differences and head-motion, the fMRI images were coregistered to the 3D (T1) anatomical image and the mean functional image; then, the images were spatially normalized to the standard stereotaxic space MNI [Evans et al., 1993]. Additionally, artifacts related to blood pulsation, head movement and instrumental spikes were removed from the BOLD time series in MNI space, using independent component analysis as implemented in GIFT [Calhoun et al., 2009; Sui et al., 2009]. No global signal regression or spatial smoothing was applied. Mean BOLD time series were extracted from the 90 regions of interest (ROIs) in the standard Automatic Anatomical Labeling (AAL) atlas [Tzourio-Mazoyer et al., 2002]. The atlas was previously masked with the binarized subjective tissue probability maps to isolate the mean value of the regions from the gray matter via a conventional protocol [Power et al., 2014; Villain et al., 2010]. The following mask was used: [Atlas * (GM > WM) * (GM > CSF) * (GM > 0.1)], where GM stands for gray matter, WM is the white matter and CSF stands for cerebrospinal fluid. Afterward, the BOLD time series for each region were band-pass filtered within the resting-state fMRI narrowband going from 0.04 to 0.07 Hz [Achard et al., 2006; Glerean et al., 2012]. A schematic representation of these steps is shown in sections A and B of Figure 1.

Statistical Analyses

Extraction of functional connectivity networks for each individual

Two different approaches were used in this study to estimate functional connectivity from the band-passed time series described above. First, a conventional approach to examine correlations between fMRI BOLD time series [ninety $x(t)$ series per individual: one for each AAL ROI] was used [Smith et al., 2013]. Briefly, the partial correlation matrix was obtained from the 90 ROIs at the 210 slices scanned over time. Partial correlation coefficients give a measure of the extent of association between two variables (i.e., every pair of ROIs) controlling for the effect of the other variables (i.e., the remaining ROIs). This step produced a 90 × 90 matrix representing the functional connectivity (FC) between each pair of brain ROIs, which was then normalized using Fischer's z transform [Fox et al., 2005; Jenkins and Watts, 1968]. Then, following a previous technical report [Schwarz and McGonigle, 2011], a soft threshold procedure was implemented to remove negative edges, as their particular network topology can drastically alter the properties of brain fMRI connectivity networks. The leftmost part of sections D and E in Figure 1 schematizes this procedure, applied to a random individual's data.

Complementarily, in view of recent reports showing a major role for the analytic components of resting-state BOLD time series in shaping the relationship between structure and function of the brain [Ponce-Alvarez et al., 2015], the time series from the 90 ROIs were further processed. Specifically, the analytic representation of the real valued signals built from the band-passed (0.04–0.07 Hz) BOLD time series was computed with the Hilbert transform. Namely, given a BOLD time series $x(t)$ for a particular ROI, its analytic representation is the complex signal

$$x_a(t) = x(t) + i\mathrm{H}[x(t)],$$

where $H[\cdot]$ is the Hilbert transform, and i stands for $\sqrt[2]{-1}$. This new signal $x_a(t)$ has the same Fourier transform as $x(t)$, but is defined only for positive frequencies. Likewise, if $x(t)$ is expressed as an amplitude-modulated signal $a(t)$ with carrier frequency $\varphi(t)$, so that $x(t) = a(t)\cos[\varphi(t)]$. Its Hilbert transform gives

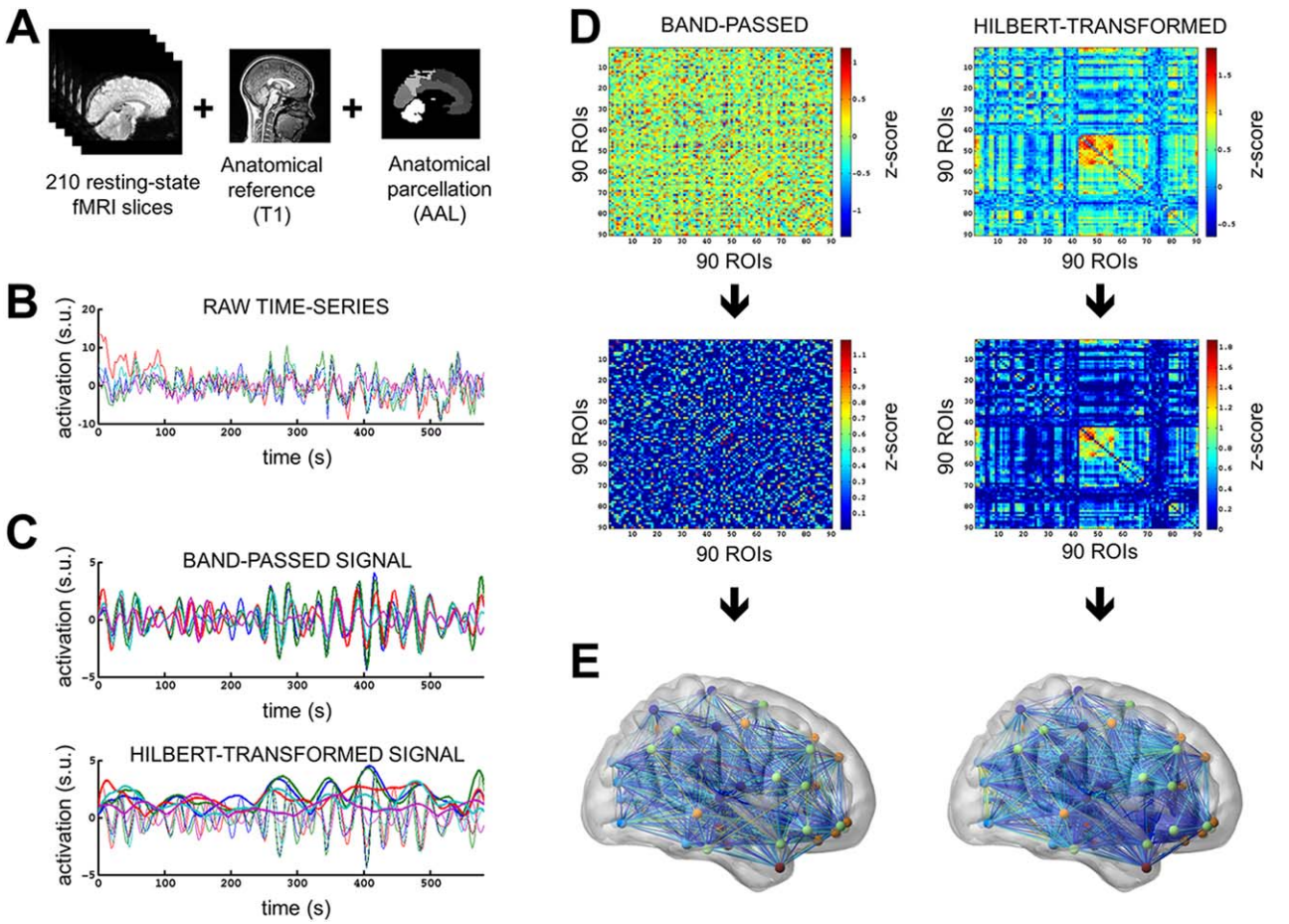

Figure 1.

Schematic representation of the construction of two functional networks for one brain. (**A**) The 210 resting-state fMRI volumes (slices) are co-registered to the anatomical T1 3D reference volume, and each voxel is mapped to one of the 90 ROIs in the AAL atlas. (**B**) After artefact removal, a time-series of the mean (BOLD) activation probability for each of the 90 ROIs is obtained. This is built upon the 210 fMRI slices acquired through 9:56 minutes of scan time. (**C**) (Top): A band-pass filter is applied to obtain the resting-state fMRI narrowband signal (0.04–0.07 Hz). (Bottom): An additional processing step to the above band-passed (0.04–0.07 Hz) time-series: the envelope extraction using the Hilbert transform. (**D**) Two partial correlation matrices are obtained from the previous time-series (band-passed and Hilbert transformed); they are z-transformed to normalize correlation values across individuals. Warm (cold) colors in these matrices represent large (small) correlation values between ROIs. The left tail of these correlation matrices (i.e., edges with negative z-scores) are set to 0 following a soft-thresholding procedure. (**E**) Graph-theoretical measures of nodal centrality are obtained for each brain region. [Color figure can be viewed in the online issue, which is available at wileyonlinelibrary.com.]

$$x_a(t) = a(t)e^{i\phi(t)},$$

where $a(t)$ represents the instantaneous envelope and $\phi(t)$ stands for the instantaneous phase. In the present study, the value of the signal envelope $a(t)$ is used to later estimate a 90 × 90 partial correlation matrix as described above, which is later z-transformed and soft-thresholded. The lowermost part of sections D and E in Figure 1 represent this procedure applied to data from one participant.

Measures of amygdalar centrality within the brain network

The AAL 90 atlas contains two amygdalar ROIs, from the left and right brain hemispheres. Graph-theoretical measures of amygdalar centrality within the brain were computed to later evaluate potential impairments amygdalar resting-stat fMRI activity within the context of the whole brain, and parsing out genetic and environmental factors. It is worth noting that there is previous evidence of differential genetic and environmental influences on

BOLD fMRI-derived graph-theoretical metrics in the brain [van den Heuvel et al., 2013], which justifies the adoption of this perspective.

Four different nodal centrality measures were separately computed for both left and right amygdala ROIs (i.e., eight independent scalars for each individual): (i) degree, (ii) betweenness centrality, (iii) local clustering coefficient, and (iv) eigenvector centrality. These four specific quantities were included in view that they have widely been studied in the literature [Borgatti and Everett, 2006], and as most nodal centrality metrics can be obtained by parameter-tuning from degree to eigenvector centrality, which represent limiting cases [Benzi and Klymko, 2015]. Due to the soft-thresholding procedure [Schwarz and McGonigle, 2011] adopted here, the weighted version of these metrics was estimated, and the centrality measures were computed using the Massachusetts Institute of Technology's *Matlab Tools for Network Analysis* toolbox [Bounova and de Weck, 2012]. Detailed mathematical descriptions of these metrics can be found elsewhere [Borgatti and Everett, 2006; Bounova and de Weck, 2012].

In the present context, these quantities represent: the number of links directly incident upon the amygdala (i, degree), how often the amygdala bridges through the shortest path between any two other nodes (ii, betweenness centrality), the extent to which the amygdala's neighbors are neighbors of each other (iii, local clustering coefficient), and the frequency of connections between the amygdala and highly connected brain regions (iv, eigenvector centrality).

Intersubject analyses: estimation of genetic and environmental influences on amygdalar resting-state activity

To determine the relationship between depression risk and both genetic and environmental factors altering amygdalar functional connectivity at rest, general linear models were executed, using a regression procedure described elsewhere [Begg and Parides, 2003], as implemented using the R's software packages *rms* and *mztwinreg* [Córdova-Palomera, 2015; Harrel, 2014; R Development Core Team, 2011]. Specifically, the logistic model

$$\mathrm{logit}(\pi_{ij}) = \beta_0 + \beta_B \mu_{i.} + \beta_W (X_{ij} - \mu_{i.})$$

is built by first obtaining estimates of both (a) familial factors (genetic plus shared environment, β_B) and (b) unique environmental influences (from nonshared events within a pair, β_W) on a graph-theoretical nodal centrality measure (i.e., degree, betweenness centrality, local clustering coefficient or eigenvector centrality). Subindex $i \in \{1, \ldots, n\}$ stands for pair number (here, $n = 24$ MZ pairs) and $j \in \{1,\ 2\}$ refers to co-twin number (randomly assigned). π_{ij} stands for the probability that co-twin j from the i-th pair has of being affected by depression. β_0 represents the intercept; $\mu_{i.} = (X_{i1} + X_{i2})/2$ is the mean nodal centrality measure of the i-th pair, and $X_{ij} - \mu_{i.}$ denotes the deviation of cotwin j from the pair's mean nodal centrality measure. In the next set of analyses, each of the four nodal centrality measures is considered in a regression model; left and right amygdalar measures (parsed out as familial and unique environmental estimates) are included in it. To control for potential confounding demographics (Table I), all analyses were adjusted for gender and age. Besides, the Huber–White method was used to adjust the variance-covariance matrix of these regression fits, to account for the non-independence of twin data (i.e., heteroskedasticity) [DeMaris, 1995; Harrel, 2014; White, 1982]. Previous reports have shown the usefulness of this between-within model to parse out familial and unique environmental factors underlying phenotypic relationships [Carlin et al., 2005; Frisell et al., 2012].

Power analysis estimations for these multiple regression models were conducted following standard protocols [Cohen, 1988; Champely, 2012]. After including all covariates, each of the above mentioned models has 4 and 71 numerator and denominator degrees of freedom. Using the conventional significance level of 0.05, the present sample has a power of 80.6% to detect moderately large effects (Cohen's $f^2 \sim 0.35$), which are expected for neuroimaging endophenotypes of brain disorders [Glahn et al., 2007; Rose and Donohoe, 2013]. However, to examine all 90 ROIs, lowering the significance level to 0.05/90—to adjust for multiple testing—would have decreased the power to 20.9%. Instead of analyzing all 90 ROIs, and given the scope and the aims of the present study, five different types of amygdalar communication mechanisms were studied in detail. This choice of biologically feasible mechanisms in hypothesis-driven research to avoid overly conservative multiple testing adjustments has previously been proposed as an adequate paradigm in epidemiological and medical statistics [Cook and Farewell, 1996; Perneger, 1998]. Exploratory *post-hoc* tests compared the number of statistical associations found for the amygdala with the results that would have been found for the other 89 ROIs (see Results and Supporting Information Figure); they suggested that the amygdala could be the most relevant ROI in this fMRI design.

Although part of the phenotypical variance of depression may be explained by gene-environment interaction effects, the current data may have limited statistical power to detect such associations [Jaccard and Wan, 1995; Jaccard et al., 1990; Mathieu et al., 2012]. Accordingly, the results presented here focus mainly on the separate influence of familial and environmental factors.

Finally, when appropriate, multiple testing adjustments of the regression coefficients from the different (independent) regression models were implemented using the false discovery rate (FDR) approach. The adoption of this Type-I error rate correction is based on previous literature of statistical analysis for biological and behavioral data [Benjamini and Hochberg, 1995; Cook and Farewell, 1996; Glickman et al., 2014; Liu et al., 2004; Nakagawa, 2004; Perneger, 1998].

TABLE II. Descriptive data of the four centrality measures analyzed for both left and right amygdalar ROIs

		Individual level (n = 48 subjects)				Intrapair differences (n = 24 MZ pairs)			
		Amplitude correlation[a]		Amplitude envelope correlation (Hilbert-transformed)[b]		Amplitude correlation[a]		Amplitude envelope correlation (Hilbert- transformed)[b]	
Nodal centrality measure	Brain hemisphere	Mean (S.D.)	Range	Mean (S.D.)	Range	Spear-man's Rho[c]	P-value	Spear-man's Rho[c]	P-value
Degree	Left	12.9 (2.3)	9.1 to 19.1	36.7 (21.9)	6.3 to 110	−0.05	0.827	0	0.991
	Right	12.5 (2)	8.7 to 15.9	32.2 (19.5)	4.4 to 88.9	−0.2	0.357	0.11	0.617
Betweenness centrality	Left	0.2 (0.2)	0 to 1.1	0.3 (0.3)	0 to 1.2	0.3	0.159	−0.22	0.308
	Right	0.3 (0.4)	0 to 1.3	0.4 (0.5)	0 to 2.3	−0.51	0.014[c]	−0.22	0.307
Local clustering coefficient	Left	0.3 (0.1)	0.2 to 0.4	0.4 (0)	0.3 to 0.5	−0.43	0.043[c]	0	0.977
	Right	0.3 (0.1)	0.2 to 0.4	0.4 (0)	0.3 to 0.5	−0.21	0.331	0.12	0.589
Eigenvector centrality	Left	0 (0.1)	−0.2 to 0.1	0 (0.1)	−0.1 to 0.2	−0.07	0.739	0.1	0.663
	Right	0 (0.1)	−0.1 to 0.1	0 (0.1)	−0.1 to 0.1	−0.09	0.682	0.05	0.834

As mentioned above (Section Extraction of functional connectivity networks for each individual), two different functional connectivity network construction procedures were employed. Namely,
[a]The conventional soft-thresholding method of band-passed low-frequency oscillations [Smith et al., 2013].
[b]The amplitude envelope extraction from the previous band-passed time-series [Glerean et al., 2012].
[c]Statistically-significant P-value. S.D., standard deviation; MZ, monozygotic.

RESULTS

As mentioned before, though scarce, there is some evidence of dissimilarities within MZ pairs for graph-theoretical measures of brain functional connectivity at rest [van den Heuvel et al., 2013]. Hence, to verify that these parameters are driven not only by genetic but also by environmental factors, a preliminary step consisted in the estimation of intrapair correlations in graph-theoretical-based connectivity measures. Table II shows these descriptive parameters.

As presented in Table II, there was an important extent of MZ intrapair differences across all these metrics, as indicated by their low and mostly nonsignificant correlation coefficients. Of note, even when there were statistically significant intrapair correlations in nodal centralities (left local clustering coefficient and right betweenness centrality in the conventional processing protocol), the correlation coefficients were moderate (Spearman's rho equaling −0.41 and −0.51, respectively). Remarkably, no statistically significant intrapair correlations are observed when the resting-state time series are Hilbert-transformed. These observations justify the ensuing procedure to parse out genetic and environmental factors underlying amygdalar resting-state activity centrality.

It is also worth noting that the nodal centrality measures computed from the amplitude envelope of the low-frequency envelope (i.e., using the Hilbert-transform of the 0.04–0.07 Hz signal) consistently showed less intrapair correlations than their non-transformed counterparts (typically smaller absolute rho and larger P-values, as displayed in Table II). This fact probably indicates that some environmental factors are cannot be straightforwardly deduced from the raw fMRI time-series but may probably be disclosed by performing different signal processing techniques such as amplitude envelope extraction.

The last set of analyses conducted here allowed the estimation of both genetic and environmental influences on amygdalar resting-state fMRI activity that may influence risk on depressive psychopathology. As indicated in Table III, the conventional brain network construction by examining the (band-pass filtered) low-frequency oscillations during rest indicated that nongenetic factors that alter amygdalar communication with the whole brain can increase depression risk. More explicitly, nongenetic factors alter left amygdalar connectivity to increase depression risk in two ways: by increasing its degree centrality and by decreasing its local clustering coefficient (i.e., left-amygdalar hypersynchronization with the rest of the brain, and less synchronization between its functional neighbors). Likewise, environmental factors may induce reductions in right-amygdalar betweenness centrality (i.e., its intermediate role in the synchrony between any two brain regions) to rise depression risk. It is important noting that these three associations between environmental factors altering amygdalar activity and depression risk should be taken with caution, as two of them were significant only at a trend level when adjusting for multiple comparisons (FDR-adjusted P-values: left degree = 0.08, left clustering coefficient = 0.02, right betweenness centrality = 0.075).

The above mentioned environmental influences on resting-state amygdalar connectivity—for both band-passed amplitude correlations and Hilbert-transformed amplitude envelope correlations—, as well as how they may influence depression risk, are depicted in Figure 2. Moreover, it is interesting noticing that the influence of familial factors on amygdalar connectivity was detected

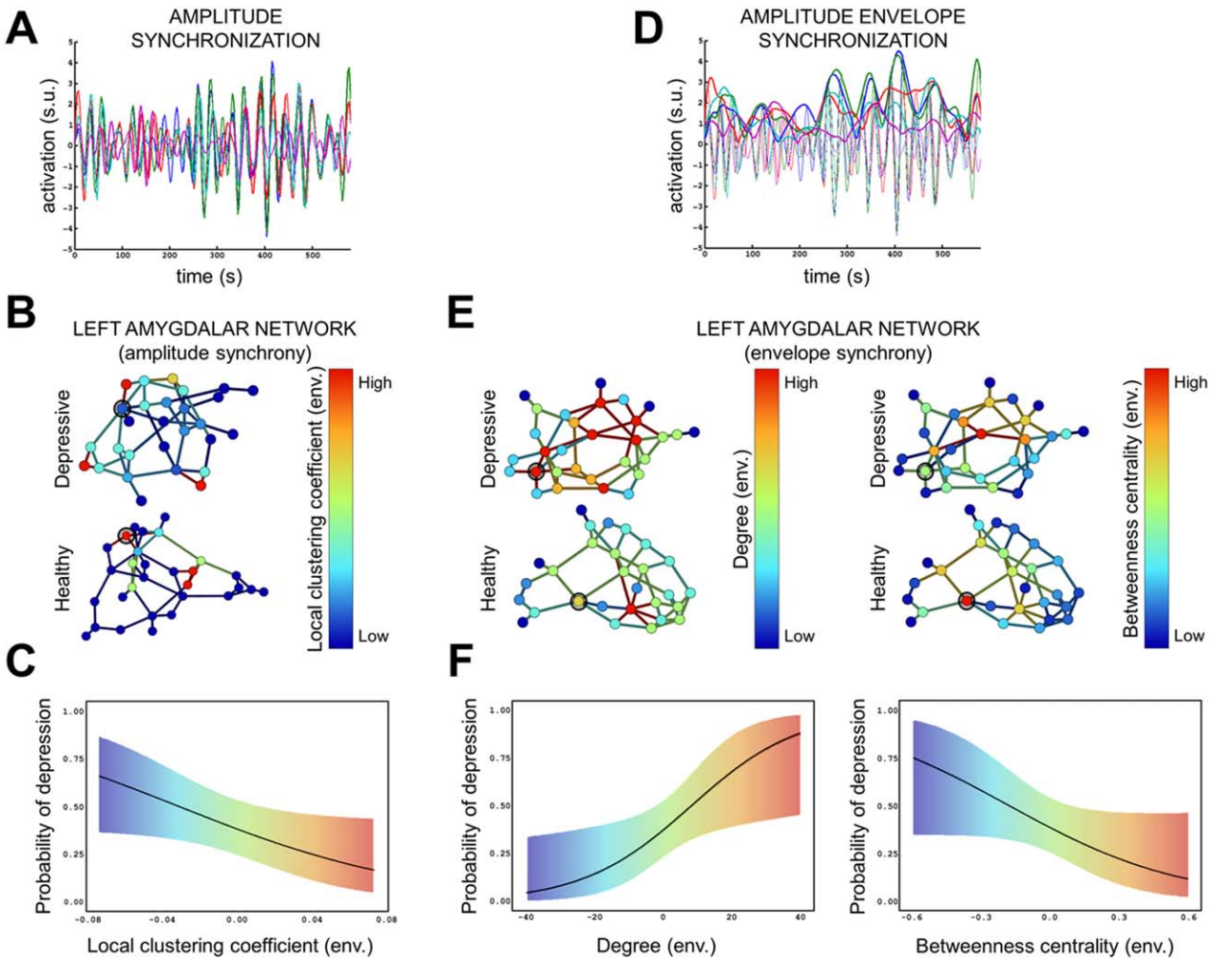

Figure 2.

Environmental factors altering resting-state amygdalar connectivity relate to depression. Only results that survived FDR multiple testing adjustments are shown. (**A**) The conventional approach to resting-state connectivity analysis, based on the estimation of a whole-brain partial correlation matrix allowed detecting environmentally-induced amygdalar connectivity alterations potentially linked to depression (as shown in sections B and C). (**B**, **C**) The environmental influences on the left amygdala (highlighted node) may decrease its local clustering coefficient to induce depression. (**D**) The amplitude envelope obtained from the Hilbert-transformed resting-state signal allowed identifying more environmentally-induced modifications of the amygdalar connectivity that could be related to depression (as shown in sections E and F). (**E**, **F**) Some environmental factors may alter the left amygdala (highlighted node) to induce depression, mainly by increasing its nodal degree (leftmost panels in E, F) and decreasing its betweenness centrality (rightmost panels in E, F). For simplicity, the logistic regression curves shown in C and F were estimated from univariate models. [Color figure can be viewed in the online issue, which is available at wileyonlinelibrary.com.]

only when computing the Hilbert-transformed amplitude envelope correlations (Fig. 3).

Notably, the additional processing step of amplitude envelope estimation using the Hilbert transform showed complementary results, with logistic regression models outperforming their conventional processing counterparts. As indicated by the better discrimination indexes obtained using amplitude envelopes (overall $R^{2\prime}$s in Table III), fMRI resting-state amygdalar centrality measures typically provide better indications of depression risk when they are derived from the Hilbert-transformed signal. This was the case when analyzing left and right amygdalar degree, betweenness centrality and local clustering coefficient. It is important mentioning that amygdalar eigenvector centrality did not seem related to depression risk in none of the models considered here.

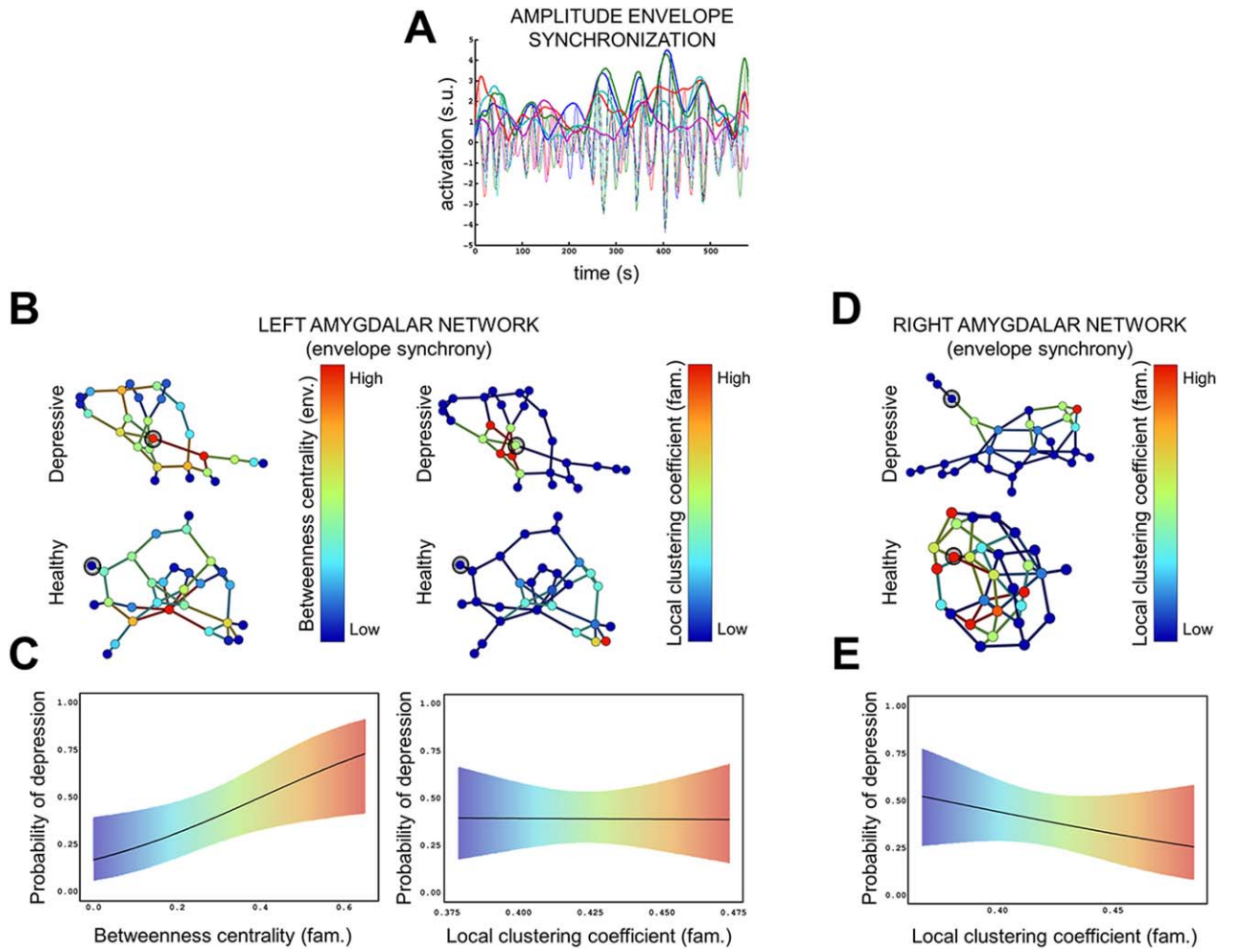

Figure 3.

Familial factors altering resting-state amygdalar connectivity relate to depression. Only results that survived FDR multiple testing adjustments are shown. (**A**) The amplitude envelope, derived from the analytical representation of resting-state fMRI signals, allowed identifying amygdalar connectivity alterations induced by familial factors (genes and shared environment) potentially linked to depression (as shown in sections B–E). (**B**, **C**) The familial influences on the left amygdala (highlighted node) may increase its betweenness centrality (leftmost panels in B, C) and decrease its local clustering coefficient (rightmost panels in B, C) to induce depression. (**D**, **E**) Some familial factors may alter the right amygdala (highlighted node) to induce depression, mainly by decreasing its local clustering coefficient. For simplicity, the logistic regression curves shown in C and E were estimated from univariate models. [Color figure can be viewed in the online issue, which is available at wileyonlinelibrary.com.]

Remarkably, the amplitude envelope of the whole-brain resting state fMRI signal confirmed the previous finding of an environmentally induced amygdalar hypersynchronization in depression (FDR-adjusted *P*-value for degree centrality = 0.007), and also suggested a role for left amygdalar betweenness centrality (FDR-adjusted *P*-value = 0.007). While the above mentioned findings mainly support the role of amygdalar connectivity alterations in mediating associations between exclusively environmental factors and depression, the results of the novel Hilbert-transform approach showed a different and very interesting property: they permitted recognizing that some familial factors (i.e., genes plus shared environment) that determine amygdalar resting-state fMRI activity are significantly contributing to the depression risk. Specifically, some familial factors seemed to alter both left and right amygdalar clustering coefficients (a measure of the synchrony among brain regions partly synchronized with the amygdala) to induce depression (FDR-adjusted *P*-values: left = 0.011, right- = 0.021). Likewise, familial factors increased both left and right amygdala's betweenness centrality in depression (FDR-adjusted *P*-values: left = 0.007, right = 0.064).

TABLE III. Estimation of the genetic and environmental influences on amygdalar resting-state activity that lead to depressive psychopathology

		Amplitude correlation[a]					Amplitude envelope correlation (Hilbert-transformed)[b]				
		Familial factors		Unique environment			Familial factors		Unique environment		
Nodal centrality measure	Brain hemisphere	β_B	*P*-value	β_W	*P*-value	Overall R^2	β_B	*P*-value	β_W	*P*-value	Overall R^2
Degree	Left	0.12	0.609	0.39	0.04[c]	0.224	0.01	0.817	0.07	0.002[d]	0.316
	Right	0.06	0.771	−0.17	0.41		0	0.985	0	0.853	
Betweenness centrality	Left	1.69	0.489	0.2	0.862	0.257	7.01	0.002[d]	−4.65	0.003[d]	0.508
	Right	−1.47	0.415	2.4	0.019[c]		2.44	0.032[c]	−0.41	0.739	
Local clustering coefficient	Left	−0.62	0.956	−18.4	0.005[d]	0.263	82.18	0.006[d]	−13.87	0.316	0.317
	Right	−2.34	0.833	4.86	0.474		−70.55	0.005[d]	12.98	0.366	
Eigenvector Centrality	Left	5.6	0.771	10.95	0.454	0.219	−7.38	0.471	2.9	0.73	0.18
	Right	−7.56	0.723	−18.73	0.222		0.13	0.992	0.5	0.937	

[a]The conventional soft-thresholding method for band-passed low-frequency oscillations [Smith et al., 2013].
[b]The amplitude envelope extraction from the previous band-passed time-series [Glerean et al., 2012].
[c]Statistically significant at unadjusted $P \leq 0.05$, but showing only a trend towards association ($P \leq 0.1$) after FDR adjustment
[d]Statistically significant before and after FDR adjustment at $P \leq 0.05$.

DISCUSSION

This study implemented a genetically-informative design to test the potential relationship between amygdalar resting-state fMRI activity and depression risk. The separate influence of familial and unique environmental factors altering the relationship between amygdalar activity and depression was analyzed using two different approaches to functional connectomics from resting-state fMRI. First, the conventional procedure to estimate temporal correlations between BOLD activity of paired brain ROIs was used to construct brain networks. Results using this method suggested that unique environmental factors modify the amygdalar resting-state activity to increase depression risk. Afterward, the amplitude envelope of the whole-brain resting-state activity patterns was computed to search for other informative patterns potentially embedded within the BOLD signal. This approach confirmed that the environment may modify the amygdalar functionality to lead to depression; it also set forth that familial factors (genes plus shared twin environment) affecting amygdalar resting-state patterns could play a role in depression risk.

The Environment and Amygdalar Centrality in the Depressed Brain

A first noteworthy result is the indication that the amygdalar degree—which here represents the extent of amygdala-whole-brain synchronization—is increased in depressed individuals. This communicational impairment somehow parallels previous findings of hypersynchronized oscillations in other pathological states. For instance, there is evidence of a decreased resting-state communicational complexity (i.e., a synchronization increase) in schizophrenia and autism [Andreou et al., 2014; Billeci et al., 2013; Sokunbi et al., 2013]; these hypersynchronized patterns have their limit expression in the neural activity of epileptic individuals [Stamoulis et al., 2010; Zhang et al., 2014b]. Of note, reduced communicational complexity, as indexed by redundant information across distinct sources, has largely been studied in other mathematical disciplines [Shannon, 1997]. The present findings are in this direction by suggesting a disease-associated overlap in the information carried by oscillations in the amygdala and in the rest of the brain. They also point out that environmental factors prompt such increased connectivity; this result was detected when analyzing the conventional resting-state time-series, and was clearer when examining their amplitude envelope synchronization (Fig. 2 and Table III).

Likewise, unique environmental factors altering left amygdalar betweenness centrality and local clustering coefficient seemed to predispose to depressive psychopathology (Fig. 2 and Table III). The potential biological meaning of these functional alterations can be interpreted as follows: first, the nodal clustering changes observed here would indicate a functional decoupling between brain regions with BOLD oscillatory patterns similar to (i.e., synchronized with) those of the amygdala. Similar local clustering coefficient alterations have been shown in the structural connectivity networks of MDD patients, across a number of limbic-emotional regions such as the left hippocampus [Qin et al., 2014]. Second, resting-state network alterations such as betweenness centrality of a number of brain regions have been found to predict depression status [Lord et al., 2012]. In the present context, these centrality disruptions may implicate a failure of the amygdala to bridge the shortest paths between pairs of synchronized nodes.

Familial Factors Altering Amygdalar Centrality in the Depressed Brain

When observing the model-fitting statistics across the distinct models considered here, the analysis of amygdalar betweenness centrality gave the best discrimination indexes ($R^2 = 0.508$; Table III). Of note, both genetic and environmental influences on left amygdalar betweenness centrality were significantly associated with depressive psychopathology, even after multiple testing adjustments.

Similarly, depression risk was associated with the familial factors altering both left and right amygdalar betweenness centrality of the Hilbert-transformed data (Fig. 3 and Table III).

The results of this study advocate for the use of analytic components of BOLD fMRI signals—such as the amplitude envelope—, particularly when studying the genetic influences leading to functional alterations of the amygdala in depression. This may have important implications considering the relevance of genetic factors such as the serotonin transporter genotype (5-HTTLPR) in modulating the amygdala during both resting-state and task-related fMRI paradigms [El-Hage et al., 2013; Li et al., 2012; Munafo et al., 2008]. The present findings suggest that the genetic bases of amygdalar activity may probably be better elicited by examining specific analytical properties of fMRI signals.

Additional Considerations

It is important mentioning that the left amygdala showed more robust statistical associations with depression than its right counterpart; most of its associations remained multiple testing adjustments. This is consistent with previous reports of partially lateralized amygdalar activity patterns at rest [Roy et al., 2009].

None of the analyses conducted here suggested a role for eigenvector centrality alterations of the amygdala in depression. As mentioned above, Benzi and Klymko [2015] have previously shown that degree and eigenvector centrality constitute limiting cases across a wide range of different nodal centrality measures, including the clustering coefficient. Though graph metrics derived from spectral graph theory (such as eigenvector-related measures) may be a landmark of brain anatomy across different species [de Lange et al., 2014], the current results suggest that such measures are not disrupted in the resting-state functional activity of the amygdala in depression. As likewise noticed, eigenvector centrality represents, in this context, the extent of synchrony between the amygdala to other highly synchronized brain regions.

Finally, some methodological limitations of this study should be noted. First, the sample size was modest; nevertheless, the associations found here (and their corresponding model fitting statistics shown in Table III) would support the presence of relatively strong effects. Likewise, the parcellation scheme adopted to construct the brain connectivity matrix was built upon the AAL atlas, which contains 90 ROIs across the whole brain. Hence, the present results are not directly comparable with other studies using different parcellation schemes. While this is certainly important, it is worth noting that it is not a problem only within the current report; choice of parcellation schemes is an important subject with large implications for brain connectomics research [de Reus and van den Heuvel, 2013]. To address this issue, future studies may combine higher-resolution neuroimaging scans with finer-grained anatomical atlases.

ACKNOWLEDGMENTS

Ximena Goldberg and Silvia Alemany contributed to sample collection. MRI technicians César Garrido and Santi Sotés also contributed to this work. The authors are indebted to the Medical Image core facility of the Institut d'Investigacions Biomèdiques August Pi i Sunyer (IDIBAPS) for the technical help.

REFERENCES

Achard S, Salvador R, Whitcher B, Suckling J, Bullmore E (2006): A resilient, low-frequency, small-world human brain functional network with highly connected association cortical hubs. J Neurosci 26:63–72.

Andreou C, Nolte G, Leicht G, Polomac N, Hanganu-Opatz IL, Lambert M, Engel AK, Mulert C (2014): Increased resting-state gamma-band connectivity in first-episode schizophrenia. Schizophr Bull: sbu121.

Begg MD, Parides MK (2003): Separation of individual-level and cluster-level covariate effects in regression analysis of correlated data. Stat Med 22:2591–602.

Benjamini Y, Hochberg Y (1995): Controlling the false discovery rate: A practical and powerful approach to multiple testing. J R Stat Soc Ser B (Methodological) 57:289–300.

Benzi M, Klymko C (2015): On the Limiting Behavior of Parameter-Dependent Network Centrality Measures. SIAM J Matrix Anal & Appl, 36:686–706.

Billeci L, Sicca F, Maharatna K, Apicella F, Narzisi A, Campatelli G, Calderoni S, Pioggia G, Muratori F (2013): On the application of quantitative EEG for characterizing autistic brain: A systematic review. Front Hum Neurosci 7:442

Blokland GA, de Zubicaray GI, McMahon KL, Wright MJ (2012): Genetic and environmental influences on neuroimaging phenotypes: A meta-analytical perspective on twin imaging studies. Twin Res Hum Genet 15:351–371.

Borgatti SP, Everett MG (2006): A graph-theoretic perspective on centrality. Soc Netw 28:466–484.

Bounova G, de Weck O (2012): Overview of metrics and their correlation patterns for multiple-metric topology analysis on heterogeneous graph ensembles. Phys Rev E 85:016117

Calhoun VD, Liu J, Adali T (2009): A review of group ICA for fMRI data and ICA for joint inference of imaging, genetic, and ERP data. NeuroImage 45:S163–S172.

Carlin JB, Gurrin LC, Sterne JA, Morley R, Dwyer T (2005): Regression models for twin studies: A critical review. Int J Epidemiol 34:1089–1099.

Cohen J (1988): Statistical Power Analysis for the Behavioral Sciences, Vol. xxi. Hillsdale, N.J.: L. Erlbaum Associates, 567 p.

Cook RJ, Farewell VT (1996): Multiplicity considerations in the design and analysis of clinical trials. J R Stat Soc Ser A (Stat Soc) 159:93–110.

Córdova-Palomera A (2015): mztwinreg: Regression Models for Monozygotic Twin Data. R package version 1.0–1. Retrieved from: http://CRAN.R-project.org/package=mztwinreg.

Cullen KR, Westlund MK, Klimes-Dougan B, Mueller BA, Houri A, Eberly LE, Lim KO (2014): Abnormal amygdala resting-state functional connectivity in adolescent depression. JAMA Psychiatry 71:1138–1147.

Champely S (2012): pwr: Basic functions for power analysis. R package version 1.1.1. Retrieved from: http://CRAN.R-project.org/package=pwr.

de Lange SC, de Reus MA, van den Heuvel MP (2014): The Laplacian spectrum of neural networks. Front Comput Neurosci 7:189

de Reus MA, van den Heuvel MP (2013): The parcellation-based connectome: Limitations and extensions. NeuroImage 80:397–404.

De Vico Fallani F, Richiardi J, Chavez M, Achard S (2014): Graph analysis of functional brain networks: Practical issues in translational neuroscience. Philos Trans R Soc London Ser B, Biol Sci 369: 20130520

DeMaris A (1995): A tutorial in logistic regression. J Marriage Family 57:956–968.

Derogatis LR, Melisaratos N (1983): The Brief Symptom Inventory: An introductory report. Psychol Med 13:595–605.

Domschke K, Reif A (2012): Behavioral genetics of affective and anxiety disorders. Curr Top Behav Neurosci 12:463–502.

Douw L, Schoonheim M, Landi D, Van der Meer M, Geurts J, Reijneveld J, Klein M, Stam C (2011): Cognition is related to resting-state small-world network topology: An magnetoencephalographic study. Neuroscience, 175:169–177.

Duncan LE, Keller MC (2011): A critical review of the first 10 years of candidate gene-by-environment interaction research in psychiatry. Am J Psychiatry 168:1041–1049.

Dutta A, McKie S, Deakin JF (2014): Resting state networks in major depressive disorder. Psychiatry Res 224:139–151.

El-Hage W, Zelaya F, Radua J, Gohier B, Alsop DC, Phillips ML, Surguladze SA (2013): Resting-state cerebral blood flow in amygdala is modulated by sex and serotonin transporter genotype. NeuroImage 76:90–97.

Esslinger C, Kirsch P, Haddad L, Mier D, Sauer C, Erk S, Schnell K, Arnold C, Witt SH, Rietschel M, Cichon S, Walter H, Meyer-Lindenberg A (2011): Cognitive state and connectivity effects of the genome-wide significant psychosis variant in ZNF804A. NeuroImage 54:2514–2523.

Evans AC, Collins DL, Mills S, Brown E, Kelly R, Peters TM (1993): 3D statistical neuroanatomical models from 305 MRI volumes. In IEEE Conference Record Nuclear Science Symposium and Medical Imaging Conference, San Francisco, CA, pp. 1813–1817.

Filippini N, MacIntosh BJ, Hough MG, Goodwin GM, Frisoni GB, Smith SM, Matthews PM, Beckmann CF, Mackay CE (2009): Distinct patterns of brain activity in young carriers of the APOE-epsilon4 allele. Proc Natl Acad Sci USA 106:7209–7214.

First MB (1997): Structured Clinical Interview for DSM-IV Axis I Disorders: SCID - I: Clinician Version: Administration Booklet. Washington, D.C.: American Psychiatric Press.

Fornito A, Zalesky A, Bassett DS, Meunier D, Ellison-Wright I, Yucel M, Wood SJ, Shaw K, O'Connor J, Nertney D, Mowry BJ, Pantelis C, Bullmore ET (2011): Genetic influences on cost-efficient organization of human cortical functional networks. J Neurosci 31:3261–3270.

Fox MD, Snyder AZ, Vincent JL, Corbetta M, Van Essen DC, Raichle, ME (2005): The human brain is intrinsically organized into dynamic, anticorrelated functional networks. Proceedings of the Natl Acad Sci USA 102:9673–9678.

Freeman HL, Stansfeld SA (2008): The Impact of the Environment on Psychiatric Disorder. London, New York: Routledge, 330 p.

Fries P (2005): A mechanism for cognitive dynamics: Neuronal communication through neuronal coherence. Trends Cogn Sci 9:474–480.

Fries P (2009): Neuronal gamma-band synchronization as a fundamental process in cortical computation. Annu Rev Neurosci 32:209–224.

Frisell T, Oberg S, Kuja-Halkola R, Sjolander A (2012): Sibling comparison designs: Bias from non-shared confounders and measurement error. Epidemiology 23:713–720.

Friston KJ, Holmes AP, Poline JB, Grasby PJ, Williams SC, Frackowiak RS, Turner R (1995): Analysis of fMRI time-series revisited. NeuroImage 2:45–53.

Glahn DC, Knowles EE, McKay DR, Sprooten E, Raventos H, Blangero J, Gottesman II, Almasy L (2014): Arguments for the sake of endophenotypes: Examining common misconceptions about the use of endophenotypes in psychiatric genetics. Am J Med Genet Part B, Neuropsychiatric Genet 165B:122–130.

Glahn DC, Thompson PM, Blangero J (2007): Neuroimaging endophenotypes: Strategies for finding genes influencing brain structure and function. Hum Brain Mapp 28:488–501.

Glahn DC, Winkler AM, Kochunov P, Almasy L, Duggirala R, Carless MA, Curran JC, Olvera RL, Laird AR, Smith SM, Beckmann CF, Fox PT, Blangero J (2010): Genetic control over the resting brain. Proc Natl Acad Sci USA 107:1223–1228.

Glerean E, Salmi J, Lahnakoski JM, Jaaskelainen IP, Sams M (2012): Functional magnetic resonance imaging phase synchronization as a measure of dynamic functional connectivity. Brain Connect 2:91–101.

Glickman ME, Rao SR, Schultz MR (2014): False discovery rate control is a recommended alternative to Bonferroni-type adjustments in health studies. J Clin Epidemiol 67:850–857.

Gottesman II, Gould TD (2003): The endophenotype concept in psychiatry: Etymology and strategic intentions. Am J Psychiatry 160:636–645.

Guggisberg AG, Rizk S, Ptak R, Di Pietro M, Saj A, Lazeyras F, Lovblad KO, Schnider A, Pignat JM (2014): Two intrinsic coupling types for resting-state integration in the human brain. Brain Topogr 28:318–329.

Guilherme R, Drunat S, Delezoide AL, Oury JF, Luton D (2009): Zygosity and chorionicity in triplet pregnancies: New data. Hum Reprod 24:100–105.

Harrel F (2014): rms: Regression Modeling Strategies. R package version 4.2-1. Retrieved from: http://CRAN.R-project.org/package=rms.

Hyde LW, Bogdan R, Hariri AR (2011): Understanding risk for psychopathology through imaging gene-environment interactions. Trends Cogn Sci 15:417–427.

Jaccard J, Wan CK (1995): Measurement error in the analysis of interaction effects between continuous predictors using multiple regression: Multiple indicator and structural equation approaches. Psychol Bull 117:348

Jaccard J, Wan CK, Turrisi R (1990): The detection and interpretation of interaction effects between continuous variables in multiple regression. Multivariate Behav Res 25: 467–478.

Jenkins GM, Watts DG (1968): Spectral Analysis and Its Applications, Vol. xviii. San Francisco: Holden-Day, 525 p.

Kaiser RH, Andrews-Hanna JR, Wager TD, Pizzagalli DA (2015): Large-scale network dysfunction in major depressive disorder: A meta-analysis of resting-state functional connectivity. JAMA Psychiatry 72:603–611.

Kendler KS, Hettema JM, Butera F, Gardner CO, Prescott CA (2003): Life event dimensions of loss, humiliation, entrapment, and danger in the prediction of onsets of major depression and generalized anxiety. Arch Gen Psychiatry 60:789–796.

Kessler RC, Angermeyer M, Anthony JC, De Graaf R, Demyttenaere K, Gasquet I, De Girolamo G, Gluzman S, Gureje O, Haro JM, Kawakami N, Karam A, Levinson D, Medina Mora ME, Oakley Browne MA, Posada-Villa J, Stein DJ, Adley Tsang CH, Aguilar-Gaxiola S, Alonso J, Lee S, Heeringa S, Pennell BE, Berglund P, Gruber MJ, Petukhova M, Chatterji S, Ustun TB (2007): Lifetime prevalence and age-of-onset distributions of mental disorders in the World Health Organization's World Mental Health Survey Initiative. World Psychiatry 6:168–176.

Lee MH, Smyser CD, Shimony JS (2013): Resting-state fMRI: A review of methods and clinical applications. AJNR. Am J Neuroradiol 34:1866–1872.

Leonardo ED, Hen R (2006): Genetics of affective and anxiety disorders. Annu Rev Psychol 57:117–137.

Li S, Zou Q, Li J, Li J, Wang D, Yan C, Dong Q, Zang YF (2012): 5-HTTLPR polymorphism impacts task-evoked and resting-state activities of the amygdala in Han Chinese. PloS One 7: e36513

Liu J, Pearlson G, Windemuth A, Ruano G, Perrone-Bizzozero NI, Calhoun V (2009): Combining fMRI and SNP data to investigate connections between brain function and genetics using parallel ICA. Hum Brain Mapp 30:241–255.

Liu J, Ren L, Womer FY, Wang J, Fan G, Jiang W, Blumberg HP, Tang Y, Xu K, Wang F (2014): Alterations in amplitude of low frequency fluctuation in treatment-naive major depressive disorder measured with resting-state fMRI. Hum Brain Mapp 35: 4979–4988.

Liu W, Jamshidian M, Zhang Y (2004): Multiple comparison of several linear regression models. J Am Stat Assoc 99:395–403.

Lord A, Horn D, Breakspear M, Walter M (2012): Changes in community structure of resting state functional connectivity in unipolar depression. PloS One 7:e41282

Lundberg A (1998): The Environment and Mental Health: A Guide for Clinicians, Vol. xi. Mahwah, N.J.: Lawrence Erlbaum Associates, 233 p.

Lynn R, Meisenberg G (2010): National IQs calculated and validated for 108 nations. Intelligence 38:353–360.

Martin AK, Robinson G, Reutens D, Mowry B (2014): Copy number deletion burden is associated with cognitive, structural, and resting-state network differences in patients with schizophrenia. Behav Brain Res 272:324–334.

Mathieu JE, Aguinis H, Culpepper SA, Chen G (2012): Understanding and estimating the power to detect cross-level interaction effects in multilevel modeling. J Appl Psychol 97:951–966.

McCabe C, Mishor Z (2011): Antidepressant medications reduce subcortical-cortical resting-state functional connectivity in healthy volunteers. NeuroImage 57:1317–1323.

Moffitt TE, Caspi A, Harrington H, Milne BJ, Melchior M, Goldberg D, Poulton R (2007): Generalized anxiety disorder and depression: Childhood risk factors in a birth cohort followed to age 32. Psychol Med 37:441–452.

Mosing MA, Gordon SD, Medland SE, Statham DJ, Nelson EC, Heath AC, Martin NG, Wray NR (2009): Genetic and environmental influences on the co-morbidity between depression, panic disorder, agoraphobia, and social phobia: A twin study. Depress Anxiety 26:1004–1011.

Munafo MR, Brown SM, Hariri AR (2008): Serotonin transporter (5-HTTLPR) genotype and amygdala activation: A meta-analysis. Biolog Psychiatry 63:852–857.

Murray CJ, Vos T, Lozano R, Naghavi M, Flaxman AD, Michaud C, Ezzati M, Shibuya K, Salomon JA, Abdalla S, Aboyans V, Abraham J, Ackerman I, Aggarwal R, Ahn SY, Ali MK, Alvarado M, Anderson HR, Anderson LM, Andrews KG, Atkinson C, Baddour LM, Bahalim AN, Barker-Collo S, Barrero LH, Bartels DH, Basanez MG, Baxter A, Bell ML, Benjamin EJ, Bennett D, Bernabe E, Bhalla K, Bhandari B, Bikbov B, Bin Abdulhak A, Birbeck G, Black JA, Blencowe H, Blore JD, Blyth F, Bolliger I, Bonaventure A, Boufous S, Bourne R, Boussinesq M, Braithwaite T, Brayne C, Bridgett L, Brooker S, Brooks P, Brugha TS, Bryan-Hancock C, Bucello C, Buchbinder R, Buckle G, Budke CM, Burch M, Burney P, Burstein R, Calabria B, Campbell B, Canter CE, Carabin H, Carapetis J, Carmona L, Cella C, Charlson F, Chen H, Cheng AT, Chou D, Chugh SS, Coffeng LE, Colan SD, Colquhoun S, Colson KE, Condon J, Connor MD, Cooper LT, Corriere M, Cortinovis M, de Vaccaro KC, Couser W, Cowie BC, Criqui MH, Cross M, Dabhadkar KC, Dahiya M, Dahodwala N, Damsere-Derry J, Danaei G, Davis A, De Leo D, Degenhardt L, Dellavalle R, Delossantos A, Denenberg J, Derrett S, Des Jarlais DC, Dharmaratne SD, Dherani M, Diaz-Torne C, Dolk H, Dorsey ER, Driscoll T, Duber H, Ebel B, Edmond K, Elbaz A, Ali SE, Erskine H, Erwin PJ, Espindola P, Ewoigbokhan SE, Farzadfar F, Feigin V, Felson DT, Ferrari A, Ferri CP, Fevre EM, Finucane MM, Flaxman S, Flood L, Foreman K, Forouzanfar MH, Fowkes FG, Fransen M, Freeman MK, Gabbe BJ, Gabriel SE, Gakidou E, Ganatra HA, Garcia B, Gaspari F, Gillum RF, Gmel G, Gonzalez-Medina D, Gosselin R, Grainger R, Grant B, Groeger J, Guillemin F, Gunnell D, Gupta R, Haagsma J, Hagan H, Halasa YA, Hall W, Haring D, Haro JM, Harrison JE, Havmoeller R, Hay RJ, Higashi H, Hill C, Hoen B, Hoffman H, Hotez PJ, Hoy D, Huang JJ, Ibeanusi SE, Jacobsen KH, James SL, Jarvis D, Jasrasaria R, Jayaraman S, Johns N, Jonas JB, Karthikeyan G, Kassebaum N, Kawakami N, Keren A, Khoo JP, King CH, Knowlton LM, Kobusingye O, Koranteng A, Krishnamurthi R, Laden F, Lalloo R, Laslett LL, Lathlean T, Leasher JL, Lee YY, Leigh J, Levinson D, Lim SS, Limb E, Lin JK, Lipnick M, Lipshultz SE, Liu W, Loane M, Ohno SL, Lyons R, Mabweijano J, MacIntyre MF, Malekzadeh R, Mallinger L, Manivannan S, Marcenes W, March L, Margolis DJ, Marks GB, Marks R, Matsumori A, Matzopoulos R, Mayosi BM, McAnulty JH, McDermott MM, McGill N, McGrath J, Medina-Mora ME, Meltzer M, Mensah GA, Merriman TR, Meyer AC, Miglioli V, Miller M, Miller TR, Mitchell PB, Mock C, Mocumbi AO, Moffitt TE, Mokdad AA, Monasta L, Montico M, Moradi-Lakeh M, Moran A, Morawska L, Mori R, Murdoch ME, Mwaniki MK, Naidoo K, Nair MN, Naldi L, Narayan KM, Nelson PK, Nelson RG, Nevitt MC, Newton CR, Nolte S, Norman P, Norman R, O'Donnell M, O'Hanlon S, Olives C, Omer SB, Ortblad K, Osborne R, Ozgediz D, Page A, Pahari B, Pandian JD, Rivero AP , Patten SB, Pearce N, Padilla RP, Perez-Ruiz F, Perico N, Pesudovs K, Phillips D, Phillips MR, Pierce K, Pion S, Polanczyk GV, Polinder S, Pope CA, 3rd, Popova S, Porrini E, Pourmalek F,

Prince M, Pullan RL, Ramaiah KD, Ranganathan D, Razavi H, Regan M, Rehm JT, Rein DB, Remuzzi G, Richardson K, Rivara FP, Roberts T, Robinson C, De Leon FR, Ronfani L, Room R, Rosenfeld LC, Rushton L, Sacco RL, Saha S, Sampson U, Sanchez-Riera L, Sanman, Schwebel DC, Scott JG, Segui-Gomez M, Shahraz S, Shepard DS, Shin H, Shivakoti R, Singh D, Singh GM, Singh JA, Singleton J, Sleet DA, Sliwa K, Smith E, Smith JL, Stapelberg NJ, Steer A, Steiner T, Stolk WA, Stovner LJ, Sudfeld C, Syed S, Tamburlini G, Tavakkoli M, Taylor HR, Taylor JA, Taylor WJ, Thomas B, Thomson WM, Thurston GD, Tleyjeh IM, Tonelli M, Towbin JA, Truelsen T, Tsilimbaris MK, Ubeda C, Undurraga EA, van der Werf, MJ, van Os J, Vavilala MS, Venketasubramanian N, Wang M, Wang W, Watt K, Weatherall DJ, Weinstock MA, Weintraub R, Weisskopf MG, Weissman MM, White RA, Whiteford H, Wiebe N, Wiersma ST, Wilkinson JD, Williams HC, Williams SR, Witt E, Wolfe F, Woolf AD, Wulf S, Yeh PH, Zaidi AK, Zheng ZJ, Zonies D, Lopez AD, AlMazroa MA, Memish ZA (2012): Disability-adjusted life years (DALYs) for 291 diseases and injuries in 21 regions, 1990-2010: A systematic analysis for the Global Burden of Disease Study 2010. Lancet 380:2197–223.

Nakagawa S (2004): A farewell to Bonferroni: The problems of low statistical power and publication bias. Behav Ecol 15:1044–1045.

O'Reilly, J (1984): Sinusoidal Carrier Modulation. Telecommunication Principles. Houte, the Netherlands: Springer Netherlands. pp. 53–66.

Oathes DJ, Patenaude B, Schatzberg AF, Etkin A (2014): Neurobiological signatures of anxiety and depression in resting-state functional magnetic resonance imaging. Biol Psychiatry 77:385–393.

Paus T (2013): How environment and genes shape the adolescent brain. Horm Behav 64:195–202.

Perneger TV (1998): What's wrong with Bonferroni adjustments. BMJ 316:1236–1238.

Ponce-Alvarez A, Deco G, Hagmann P, Romani GL, Mantini D, Corbetta M (2015): Resting-state temporal synchronization networks emerge from connectivity topology and heterogeneity. PLoS Comput Biol 11:e1004100.

Power JD, Mitra A, Laumann TO, Snyder AZ, Schlaggar BL, Petersen SE (2014): Methods to detect, characterize, and remove motion artifact in resting state fMRI. NeuroImage 84:320–341.

Qin J, Wei M, Liu H, Yan R, Luo G, Yao Z, Lu Q (2014): Abnormal brain anatomical topological organization of the cognitive-emotional and the frontoparietal circuitry in major depressive disorder. Magn Reson Med 72:1397–1407.

R Development Core Team (2011): R: A Language and Environment for Statistical Computing. Vienna, Austria: R Foundation for Statistical Computing.

Ressler KJ, Mayberg HS (2007): Targeting abnormal neural circuits in mood and anxiety disorders: From the laboratory to the clinic. Nat Neurosci 10:1116–1124.

Richiardi J, Eryilmaz H, Schwartz S, Vuilleumier P, Van De Ville D (2011): Decoding brain states from fMRI connectivity graphs. NeuroImage 56:616–626.

Rose EJ, Donohoe G (2013): Brain vs behavior: An effect size comparison of neuroimaging and cognitive studies of genetic risk for schizophrenia. Schizophrenia Bull 39:518–526.

Roy AK, Shehzad Z, Margulies DS, Kelly AM, Uddin LQ, Gotimer K, Biswal BB, Castellanos FX, Milham MP (2009): Functional connectivity of the human amygdala using resting state fMRI. NeuroImage 45:614–626.

Rudie JD, Hernandez LM, Brown JA, Beck-Pancer D, Colich NL, Gorrindo P, Thompson PM, Geschwind DH, Bookheimer SY, Levitt P, Dapretto M (2012): Autism-associated promoter variant in MET impacts functional and structural brain networks. Neuron 75:904–915.

Ruiperez M, Ibáñez MI, Lorente E, Moro M, Ortet G (2001): Psychometric properties of the Spanish version of the BSI: Contributions to the relationship between personality and psychopathology. Eur J Psychol Assess 17:241

Sattler JM (2001): Assessment of children: Cognitive applications. San Diego: J.M. Sattler.

Schwarz AJ, McGonigle J (2011): Negative edges and soft thresholding in complex network analysis of resting state functional connectivity data. NeuroImage 55:1132–1146.

Shannon CE (1997): The mathematical theory of communication. 1963. M.D. Comput: Comput Med Practic 14:306–317.

Sheline YI, Barch DM, Price JL, Rundle MM, Vaishnavi SN, Snyder AZ, Mintun MA, Wang S, Coalson RS, Raichle ME (2009): The default mode network and self-referential processes in depression. Proc Natl Acad Sci USA 106:1942–1947.

Sheline YI, Price JL, Yan Z, Mintun MA (2010): Resting-state functional MRI in depression unmasks increased connectivity between networks via the dorsal nexus. Proc Natl Acad Sci USA 107:11020–11025.

Smith SM (2012): The future of FMRI connectivity. NeuroImage 62:1257–1266.

Smith SM, Vidaurre D, Beckmann CF, Glasser MF, Jenkinson M, Miller KL, Nichols TE, Robinson EC, Salimi-Khorshidi G, Woolrich MW, Barch DM, Ugurbil K, Van Essen DC (2013): Functional connectomics from resting-state fMRI. Trends Cogn Sci 17:666–682.

Sokunbi MO, Fung W, Sawlani V, Choppin S, Linden DE, Thome J (2013): Resting state fMRI entropy probes complexity of brain activity in adults with ADHD. Psychiatry Res 214:341–348.

Stamoulis C, Gruber LJ, Chang BS (2010): Network dynamics of the epileptic brain at rest. In: Conference Proceedings: Annual International Conference of the IEEE Engineering in Medicine and Biology Society. pp 150–153.

Sui J, Adali T, Pearlson GD, Calhoun VD (2009): An ICA-based method for the identification of optimal FMRI features and components using combined group-discriminative techniques. NeuroImage 46:73–86.

Sullivan PF, Neale MC, Kendler KS (2000): Genetic epidemiology of major depression: Review and meta-analysis. Am J Psychiatry 157:1552–1562.

Trachtenberg AJ, Filippini N, Ebmeier KP, Smith SM, Karpe F, Mackay CE (2012): The effects of APOE on the functional architecture of the resting brain. NeuroImage 59:565–572.

Tunbridge EM, Harrison PJ, Weinberger DR (2006): Catechol-o-methyltransferase, cognition, and psychosis: Val158Met and beyond. Biol Psychiatry 60:141–151.

Tzourio-Mazoyer N, Landeau B, Papathanassiou D, Crivello F, Etard O, Delcroix N, Mazoyer B, Joliot M (2002): Automated anatomical labeling of activations in SPM using a macroscopic anatomical parcellation of the MNI MRI single-subject brain. NeuroImage 15:273–289.

van den Heuvel MP, Hulshoff Pol HE (2010): Exploring the brain network: A review on resting-state fMRI functional connectivity. Eur Neuropsychopharmacol 20:519–534.

van den Heuvel MP, van Soelen IL, Stam CJ, Kahn RS, Boomsma DI, Hulshoff Pol HE (2013): Genetic control of functional brain network efficiency in children. Eur Neuropsychopharmacol 23:19–23.

Villain N, Fouquet M, Baron JC, Mezenge F, Landeau B, de La Sayette V, Viader F, Eustache F, Desgranges B, Chetelat G (2010): Sequential relationships between grey matter and white matter atrophy and brain metabolic abnormalities in early Alzheimer's disease. Brain 133:3301–3314.

Wang L, Dai Z, Peng H, Tan L, Ding Y, He Z, Zhang Y, Xia M, Li Z, Li W, Cai Y, Lu S, Liao M, Zhang L, Wu W, He Y, Li L (2014): Overlapping and segregated resting-state functional connectivity in patients with major depressive disorder with and without childhood neglect. Hum Brain Mapp 35:1154–1166.

Wang L, Song M, Jiang T, Zhang Y, Yu C (2011): Regional homogeneity of the resting-state brain activity correlates with individual intelligence. Neurosci Lett 488:275–278.

Wechsler D, Cordero Pando A, Yela Granizo M, Zimmerman IL, Woo-Sam JM, Glasser AJ (1997): WAIS escala de inteligencia de Wechsler para adultos. Madrid, Barcelona: TEA Ediciones.

White H (1982): Maximum likelihood estimation of misspecified models. Econometrica: J Econometric Soc 50:1–25.

Wittchen HU, Kessler RC, Beesdo K, Krause P, Hofler M, Hoyer J (2002): Generalized anxiety and depression in primary care: Prevalence, recognition, and management. J Clin Psychiatry 63 Suppl 8:24–34.

Zbozinek TD, Rose RD, Wolitzky-Taylor KB, Sherbourne C, Sullivan G, Stein MB, Roy-Byrne PP, Craske MG (2012): Diagnostic overlap of generalized anxiety disorder and major depressive disorder in a primary care sample. Depression Anxiety 29:1065–1071.

Zeng LL, Shen H, Liu L, Hu D (2014): Unsupervised classification of major depression using functional connectivity MRI. Hum Brain Mapp 35:1630–1641.

Zeng LL, Shen H, Liu L, Wang L, Li B, Fang P, Zhou Z, Li Y, Hu D (2012): Identifying major depression using whole-brain functional connectivity: A multivariate pattern analysis. Brain 135: 1498–507.

Zhang X, Zhu X, Wang X, Zhu X, Zhong M, Yi J, Rao H, Yao S (2014a): First-episode medication-naive major depressive disorder is associated with altered resting brain function in the affective network. PloS One 9:e85241.

Zhang Z, Liao W, Wang Z, Xu Q, Yang F, Mantini D, Jiao Q, Tian L, Liu Y, Lu G (2014b): Epileptic discharges specifically affect intrinsic connectivity networks during absence seizures. J Neurol Sci 336:138–145.